Finite-size scaling study of two-dimensional surface growth models

1990 J. Phys. A: Math. Gen. 23 4525

(http://iopscience.iop.org/0305-4470/23/20/014)

J. Phys. A: Math. Gen. **23** (1990) 4525-4536. Printed in the UK

Finite-size scaling study of two-dimensional surface growth models

K Uzelac† and R Jullien‡

† Institute of Physics, University of Zagreb, POB 304, 41001 Zagreb, Croatia, Yugoslavia
‡ Laboratoire de Physique des Solides, Université Paris-Sud, Centre d'Orsay, 91405 Orsay, France

Received 23 April 1990

Abstract. A simple finite-size scaling method for two-dimensional surface growth models with restricted step heights is proposed. A master equation is written for the time evolution of the surface configuration probabilities in which enter model-dependent inter-configuration rates. These equations are numerically solved for finite systems of increasing sizes and the exponents governing the time evolution of the surface thickness are extracted using finite-size scaling analysis. The method is used to study crossovers in realistic models for ballistic deposition.

1. Introduction

Surface growth processes are phenomena of considerable scientific interest with a broad range of practical applications. These studies were pioneered by Vold [1] and Eden [2] thirty years ago, and recently re-activated as a result of the general interest in non-equilibrium growth such as aggregation [3] and random deposition [4] processes. One of the simplest models, called 'ballistic deposition', considers, in its two-dimensional version, a basal horizontal line of length L on which particles are deposited, one after another, along randomly positioned vertical trajectories. Particles become part of the deposit at their positions of first contact (nearest-neighbour contact when on lattice). This model has been extensively studied both on- [5] and off-lattice [6]. To analyse the evolution of the surface thickness ξ with time t, the following dynamical scaling has been proposed [7]:

$$\xi \sim L^{\alpha} f\left(\frac{t}{L^{\gamma}}\right). \tag{1}$$

The scaling function $f(x)$ satisfies $f(x) \to$ constant when $x \to \infty$ and $f(x) \sim x^{\beta}$, with $\beta = \alpha/\gamma$, when $x \to 0$. Hence, the scaling behaviour of ξ is different with L for large t, $\xi \sim L^{\alpha}$, than with t for large L, $\xi \sim t^{\beta}$. The most accurate numerical estimates [5] of α, β and γ, in two dimensions, are very close to $\alpha = \frac{1}{2}$, $\beta = \frac{1}{3}$ and $\gamma = \frac{3}{2}$. Realistic extensions of this model were considered in which possible surface diffusion [8], particle restructuring [6], or reversibility [9] were introduced. When a complete restructuring (the particles are allowed to slide on the surface until they reach the nearest local minimum) or a complete reversibility (the particles are allowed to evaporate or stick with symmetric rules) are considered, it is found that the scaling form (1) is still valid, but with a different γ exponent, $\gamma = 2$, while α remains equal to $\frac{1}{2}$ [6, 9]. It is

0305-4470/90/204525+12$03.50

now generally believed that such models are discrete versions of the continuous model introduced by Edwards and Wilkinson [10] ($\gamma = 2$) and subsequently modified by Kardar, Parisi and Zhang (KPZ) [11] ($\gamma = \frac{3}{2}$).

Most of the previous results on discrete models were obtained by means of Monte Carlo numerical calculations on large samples. However it has been shown that, when considering restricted step heights, the models can be mapped on simple spin models [5, 9] so that the numerical methods commonly used for spin or fermion systems can be applied. In this paper, we show how the finite-size scaling method, which is a standard tool for spin systems [12] can be applied to surface growth problems. The idea is to solve exactly the problem for small values of L and try to extrapolate the results to the infinite size. Recent results [13] showing that there are fewer finite size corrections to scaling in restricted height steps models, yield some confidence in the applicability of the finite-size method to these cases. Here, we give some examples of applications in two dimensions. Extensions to three dimensions will be presented later.

2. Principles of the calculation

In this paper we are always considering growth of a one-dimensional surface on a two-dimensional square lattice, with periodic boundary conditions at the edges of a strip of L columns, with L even. To reduce the number of surface configurations, we only allow steps of one unit length, positive or negative, between the surface heights, h_l of neighbouring columns. As already noticed [5], a given surface configuration can be represented by a set of L spin variables $(s_1, s_2, \ldots, s_L)$, with $s_l = h_l - h_{l-1} = \pm 1$, where $l = 1, 2, \ldots, L$ labels the step between columns $l-1$ and l. Periodic boundary conditions impose that the total 'magnetization', $m = \Sigma_l s_l$, should be zero so that the total number of distinct configurations, Ω, is given by

$$\Omega = \frac{L!}{[(L/2)!]^2}. \tag{2}$$

Conventionally, we call a flat surface, a surface which is in configuration $(+, -, +, -\ldots)$ or $(-, +, -, +\ldots)$ with equal probability.

Starting with a flat surface, our growth models will generate with the same probabilities those configurations which belong to the same symmetry class. Here a symmetry class is defined by the invariance to cyclic permutations and to reflection (in the spin picture, the reflection implies also a spin-flip transformation in the same time). Note, however, that a global particle-hole symmetry (spin-flip alone) is in general not preserved by irreversible growth models. Taking care of the symmetries, it is more convenient to group the configurations into basic 'states', hereafter labelled by index i, each state representing a surface in any of the congfigurations generated from a given one using all the symmetries, with the same probability. We call the 'degeneracy' of the basic state i the number g_i of independent configurations it contains. g_i is at most equal to $2L$, otherwise it is necessarily a divisor of $2L$ and one has:

$$\sum_{i=1}^{N} g_i = \Omega \tag{3}$$

where N is the total number of basic states. In the following, the state 1, with $g_1 = 2$, corresponds to the flat surface. The example $L = 8$, where $N = 9$, is depicted in figure 1. For larger L values, the search for the basic states and the evaluation of the g_i's is

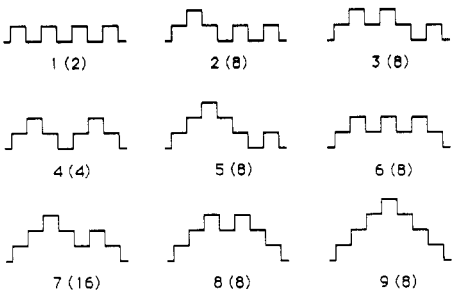

Figure 1. The $N=9$ basic states in the case $L=8$. Only one configuration per state is shown, the others can be generated using reflection and cyclic permutations. The number of independent configurations, g_i, for each state i is shown in parenthesis.

directly done by the computer, using a systematic generation of the different configurations. In the examples reported below, we went up to $L=18$, where $N=1480$.

Knowing the basic states, a growth model can be defined giving the probability rates $\Gamma_{i\to j}$ to evolve from state i at time t to state j at time $t+1$. Then, defining the probability $p_i(t)$ to be in state i at time t, the p_i's should satisfy the following master equations:

$$p_i(t+1)=p_i(t)+\Delta\left(\sum_j \Gamma_{j\to i}p_j(t)-p_i(t)\sum_j \Gamma_{i\to j}\right). \tag{4}$$

In this formula, we have introduced a constant Δ, which fixes the choice of the time unit. These equations allow to calculate the $p_i(t)$'s at any time t starting from the flat surface, i.e. $p_i(0)=1$ for $i=1$ and $p_i(0)=0$ for $i>1$. Note that the normalization of the p_i's,

$$\sum_i p_i(t)=1 \tag{5}$$

is automatically perserved by equation (4). Then, knowing the p_i's, one can calculate the time-evolution of any averaged quantity, such as the square of the surface thickness, ξ, using:

$$\xi^2(t)=\sum_i p_i(t)\xi_i^2 \tag{6}$$

ξ_i is the i-dependent surface thickness, which is the same in all configurations of the basic state i, and which is calculated by:

$$\xi_i^2=\frac{1}{L}\sum_l (h_l-h)^2-\frac{1}{4} \tag{7a}$$

with:

$$h=\frac{1}{L}\sum_l h_l. \tag{7b}$$

Note the difference with the usual definition: in (7*a*) we have arbitrarily subtracted $\frac{1}{4}$ to ensure $\xi_1=0$ for the flat surface.

Another quantity of interest, which has not been so closely considered in this context up to now, is the entropy $S(t)$, which can be calculated by:

$$S(t) = \sum_i p_i(t) \log\left(\frac{g_i}{p_i(t)}\right). \tag{8a}$$

In practice, we prefer to use a reduced entropy, $s(t)$

$$s(t) = \frac{S(t)}{\log \Omega} \tag{8b}$$

which is equal to unity at equilibrium, when all surface configurations are equiprobable, i.e. when $p_i = g_i/\Omega$.

3. Definitions of the growth models used

We have first considered, as a test, a model equivalent to the one already studied by Plischke *et al* [9]. This is an Eden-like model in which the only active columns are those corresponding to minima (i.e. l-values such that $s_l = -1$ and $s_{l+1} = +1$) and where, per unit time, a new particle can be added to any active column with equal probability. When the new particle is added at site l, the two spins s_l and s_{l+1} are flipped (note that, as in [5], this corresponds to consider rectangular particles of width 1 and height 2). When a state i is transformed into a state j, the rate $\Gamma^{(0)}_{i\to j}$ can be calculated as being the number of active sites of a configuration belonging to a state i and giving a configuration belonging to j. By definition, one has $\Sigma_j \Gamma^{(0)}_{i\to j} = \nu_i$, where ν_i is the total number of active columns (i.e. the number of minima) in a configuration of state i.

A symmetric 'disaggregation' model can be defined in which the active columns are now those corresponding to the maxima and where particles are suppressed in any active column with equal probability. The rates $\Gamma^{(1)}_{i\to j}$ for this disaggregation model correspond to the ones of the other after performing a particle-hole (=spin-flip) exchange of the states. Then, introducing a concentration c_1, one can consider, as in [9], a partially reversible model for which:

$$\Gamma_{i\to j} = (1 - c_1)\Gamma^{(0)}_{i\to j} + c_1\Gamma^{(1)}_{i\to j}. \tag{9}$$

This model will be called model (1) in the following. The case $c_1 = \frac{1}{2}$ corresponds to the completely reversible case.

We have also considered another modification of the Eden model described above to try to approach closer to realistic ballistic models with restructuring introduced earlier [6]. We consider that the new particle can fall in any column, equiprobably: when it falls on a minimum ($s_l = -s_{l+1} = -1$) we proceed as above but when it falls on a slope ($s_l = s_{l+1}$) it slides down to reach the nearest minimum, and when it falls on a maximum ($s_l = -s_{l+1} = +1$) it reaches the minimum on the right or on the left with equal probability. The rates $\Gamma^{(2)}_{i\to j}$ for this ballistic model can be calculated by assigning to each interconfiguration channel a weight equal to the width of the 'attractive basin' of the corresponding active column and then adding the contributions coming from different active columns if they lead to the same final state. Here one has $\Sigma_j \Gamma^{(2)}_{i\to j} = L$. To make this more precise, the values of the $\Gamma^{(2)}_{i\to j}$'s, together with those of the $\Gamma^{(0)}_{i\to j}$'s, in the case $L = 8$, are listed in table 1. Then, to study the crossover between Eden and

Table 1. List of the basic states in the case $L = 8$ (see figure 1). For each state we give its spin representation, its degeneracy (g_i), its surface thickness (ξ_i), the corresponding state after a spin-flip transformation, the list of the corresponding j values which yield to non-zero rates $\Gamma^{(0)}_{i\to j}$ and $\Gamma^{(2)}_{i\to j}$, and the values for these rates.

i	Spin representation	g_i	ξ_i^2	s.f. (i)	j	$\Gamma^{(0)}_{i\to j}$	$\Gamma^{(2)}_{i\to j}$
1	+−+−+−+−	2	0	1	2	4	8
2	++−−+−+−	8	0.1875	6	3	2	6
					4	1	2
3	++−+−−+−	8	0.25	3	5	1	2
					6	2	6
4	++−−++−−	4	0.25	4	6	2	8
5	+++−−−+−	8	0.6875	8	7	2	8
6	++−+−+−−	8	0.1875	2	1	1	4
					7	2	4
7	+++−−+−−	16	0.5	7	2	1	5
					8	1	3
8	+++−+−−−	8	0.6875	5	3	1	6
					9	1	2
9	++++−−−−	8	1.25	9	5	1	8

ballistic growth, we have introduced a concentration c_2 and considered the following rates:

$$\Gamma_{i\to j} = (1 - c_2)\Gamma^{(0)}_{i\to j} + c_2\Gamma^{(2)}_{i\to j}. \tag{10}$$

This model is called model (2) in the following.

In the calculations that we have performed on these two models, the i-dependent quantities such as the ξ_i's and the $\Gamma_{i\to j}$'s are calculated by the computer during the generation of the basic states. Note that the $\Gamma_{i\to j}$'s are probability rates and not probabilities so that they can all be multiplied by a constant without changing the physics, this arbitrary constant being included in the parameter Δ. In practice the choice for Δ plays some role in the numerical computation. The convergence of equation (4) is better for smaller Δ values. While the L-dependent results depend slightly on Δ, their convergence to the infinite size does not. In all the calculations reported below, with the choice of the $\Gamma_{i\to j}$'s adopted above, we have taken $\Delta = 0.1/L$.

4. Numerical results and discussion

In figures 2(a) and 2(b), we give the results for $\log \xi(t)$ and $s(t)$ as a function on $\log t$ in the Eden case, i.e. for $c_1 = c_2 = 0$. For ξ, we recover all the features expected from equation (1), i.e. a linear behaviour with slope β followed by a L-dependent saturation yielding to exponent α. In fact, we recover the saturation value, ξ_∞ which has been previously calculated analytically in this model [9]:

$$\xi_\infty = \sqrt{\frac{L-2}{12}} \tag{11}$$

and which gives exactly $\alpha = \frac{1}{2}$ (when comparing this result with reference [9], one must take care of the $\frac{1}{4}$ term in equation (7a)). The analytical calculation is made possible

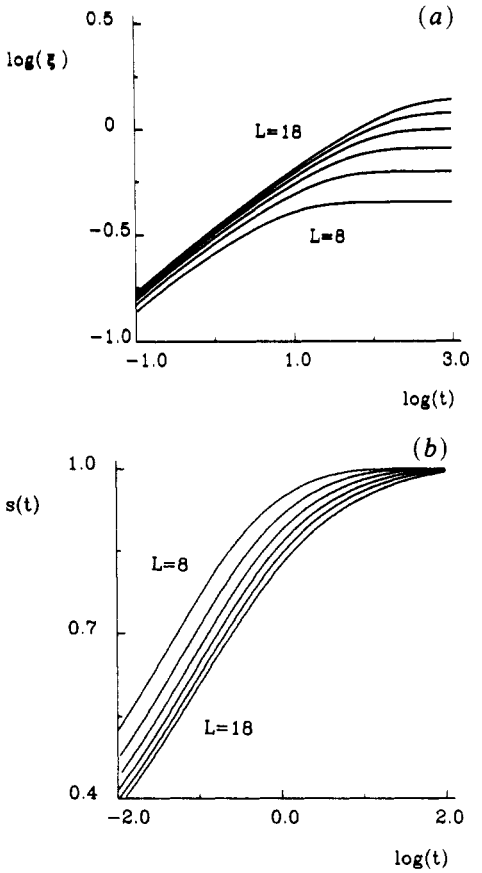

Figure 2. Plot for $\log \xi$ (a) and $s(t)$ (b) as a function of $\log t$ in the Eden case (model (1) with $c_1 = 0$ or model (2) with $c_2 = 0$).

because, in this model, the rates insure an equally weighted one-to-one correspondence between all the individual configurations so that the solution in the steady-state regime of equation (4) is exactly the equilibrium solution $p_i = g_i/\Omega$. This is also verified on the results of figure 2(b) since $s(t)$ tends to one in the saturation regime. This allows, in this case, to interpret the growth model as a classical relaxion to equilibrium. We have observed that this remains true for all concentrations in the case of model (1). In the reversible case, $c_1 = 0.5$, the curves reported in figure 3 exhibit the same qualitative behaviour. Except the low time part of $\xi(t)$ which is different and described by another β exponent, the saturation value is also given by equation (11) and $s(t)$ tends to one when t tends to infinity.

Such behaviour is no longer observed in model (2). As soon as c_2 is different from zero the saturation value ξ_∞ is different from that of equation (10) and $s(t)$ no longer tends to one. However, we have checked that the L-dependence of ξ_∞ is always consistent with $\alpha = \frac{1}{2}$. This can be seen in figure 4 and in table 2 where the results for model (2), in the case $c_2 = 1$, are reported. It is worth noticing that in this case ($c_2 = 1$) the limiting value for the entropy decreases as L increases, so that the corresponding model cannot be viewed as a relaxation process to equilibrium, even in the asymptotic limit.

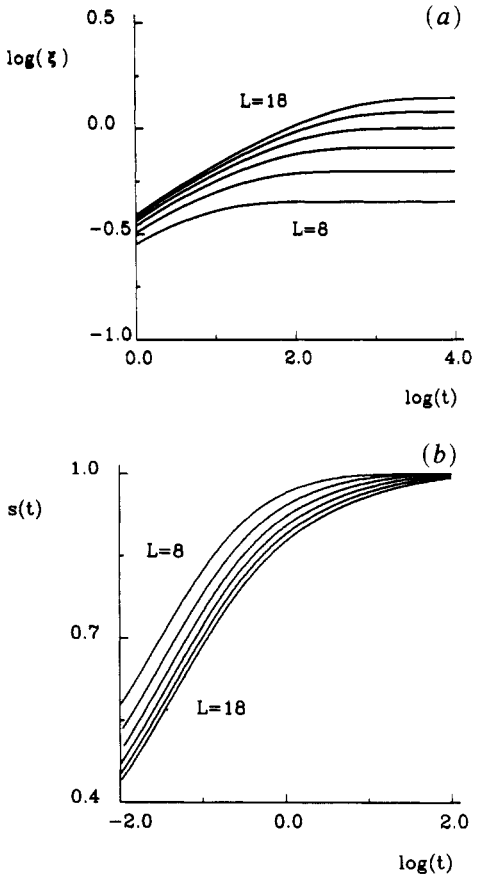

Figure 3. Plot of $\log \xi$ (a) and $s(t)$ (b) as a function of $\log \tau$ in the reversible case (model (1) with $c_1 = 0.5$).

To estimate the other exponents β and γ, which are related by $\beta = \alpha/\gamma = 0.5/\gamma$ we could have taken advantage of the low-t part of the $\xi(t)$-curves to get β, but we found that this method is not reliable in our case where, for the small L-values used, the low-t linear region is not sufficiently well developed. We have preferred to use, instead, a simple method which consists of estimating directly γ but which would have been more difficult to use with Monte Carlo data. For a finite system, the relaxation is of exponential form, and fitting $\xi(t)$, by $A + B\exp(-t/\tau)$, one can calculate a L-dependent relaxation time $\tau(L)$, which, according to (1), should behave as L^{γ} for large L. Examples of numerical results for $\tau(L)$ are given in tables 2 and 3. Then, as in usual finite-size scaling methods [12], by comparing successive sizes, $L-2$ and L, one can calculate an L-dependent effective exponent:

$$\gamma_L = \frac{\log \tau(L)/\tau(L-2)}{\log(L-2)/(L-4)} \tag{12}$$

(guided by formula (11) we have used $L-2$ and $L-4$ instead of L and $L-2$ in the denominator) which should tend to the true γ exponent when L tends to infinity. The same method can be applied to $s(t)$ instead of $\xi(t)$: we have checked it gives the same results. Note that such procedure corresponds to study the L-dependence of the gap

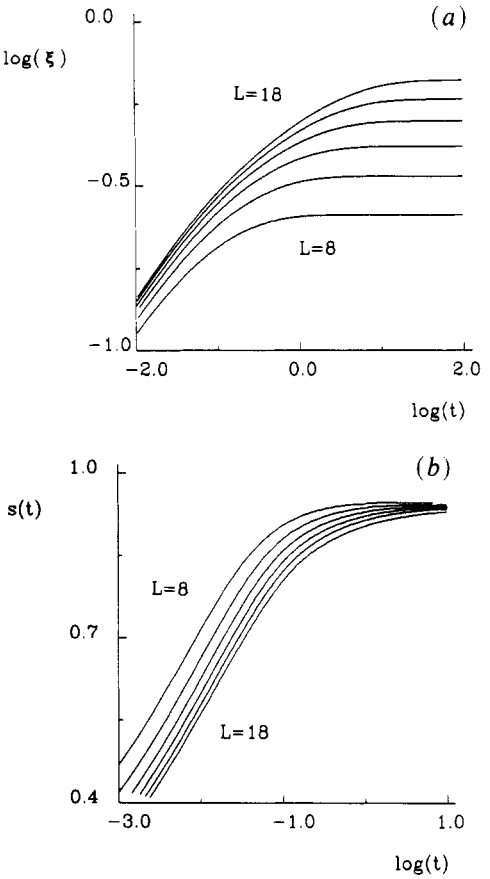

Figure 4. Plot of $\log \xi$ (a) and $s(t)$ (b) as a function of $\log t$ in the ballistic case (model (2) with $c_2 = 1$).

Table 2. Numerical results for ξ_x^2, s_x, $\tau(L)$ in the case of model (2) for $c_2 = 1$.

L	ξ_x^2	s_x	$\tau(L)$
8	0.309	0.947	4.396
10	0.390	0.944	3.123
12	0.469	0.941	2.287
14	0.547	0.939	1.731
16	0.623	0.937	1.349
18	0.700	0.935	1.078

between the two lowest eigenstates of the evolution matrix

$$H_{ij} = \Gamma_{j\to i} - \delta_{ij} \sum_k \Gamma_{i\to k}. \tag{13}$$

This idea was already used to find an exact solution of a similar model [14].

Our results for γ are given in figures 5(a) and (b), for model (1) and (2) respecitvely, where γ_L has been plotted as a function of $1/(L-3)$ for different c_1 and c_2 values. For model (1) we only report results for c_1 ranging from 0 to 0.5 since the results are the

Table 3. Numerical results for $\tau(L)$ in the case of model (1) for $c_1 = 0$ and $c_1 = 0.5$.

L	$\tau(L)$ for $c_1 = 0$	$\tau(L)$ for $c_1 = 0.5$
8	0.937	0.757
10	0.640	0.469
12	0.471	0.318
14	0.364	0.229
16	0.292	0.173
18	0.241	0.135

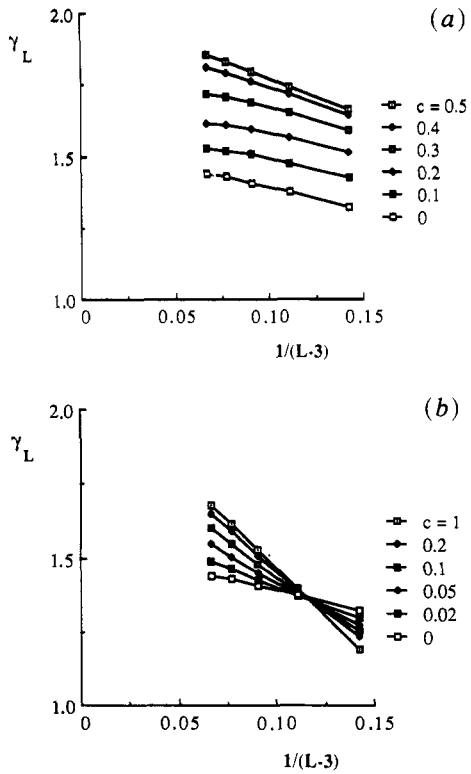

Figure 5. Plot of γ_L as a function of $1/(L-3)$, for different c-values. (a) and (b) correspond to model (1) and model (2), and the c-values correspond to c_1 and c_2, respectively.

same by changing c_1 in $1 - c_1$. While the curve for $c_1 = 0$ converges to $\gamma = 1.5$, the curve for $c_1 = 0.5$ converges to $\gamma = 2$. For all intermediate c_1 values, one observes a clear negative curvature, consistent with a convergence to $\gamma = 1.5$. This is in agreement with the conclusion of Plishke *et al* [7] that the reversible model is an unstable fixed point.

In the case of model (2) the results are consistent with $\gamma = 2$ for $c_2 = 1$. This is in good agreement with what is known on the ballistic model with complete restructuring [6]. However the crossover is the opposite of the one observed in figure 5(a). While γ_L converges to $\gamma = 1.5$ for $c_2 = 0$, it seems to converge to $\gamma = 2$ as soon as c_2 is slightly increased above $c_2 = 0$. Thus, it appears that the $\gamma = 2$ fixed point is reached as soon as there is some partial restructuring. This last result appears to be in conflict with theoretical predictions [17, 18] based on the renormalization group analysis of the

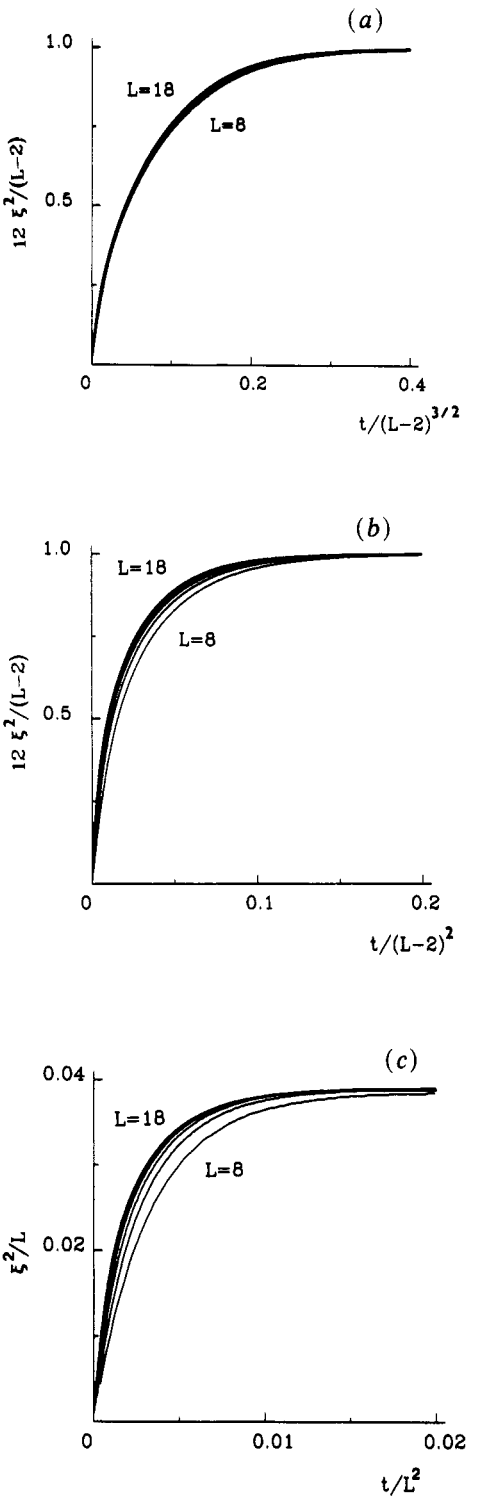

Figure 6. Scaled curves for the surface thickness. Cases (*a*), (*b*) and (*c*) correspond to figures 2, 3, 4, i.e. the Eden, reversible and ballistic case, respectively.

KPZ equation [11], for which the $\gamma = 2$ fixed point should be always unstable. However, we have already observed that introducing one step surface diffusion in the ballistic model built on lattice gives the same result ($\gamma = 2$) as a complete restructuring (the ballistic model with one step restructuring is equivalent to the independent column model with one step restructuring studied by Family [8]). This apparent discrepancy between lattice models and the continuous KPZ equation needs further attention. It might be that infinitesimally small restructuring can never be tuned on lattice or that our parameter c_2 does not vary continuously with the parameters of the KPZ equation. It is also quite possible that the crossover expected from theory occurs for length scales longer than those analysed here.

Knowing both α and γ it is possible to draw the $\xi(t)$ curves under a scaled form according to (1). This has been done in figure 6 in the three limiting cases, Eden, reversible and ballistic (with restructuring), which correspond to figures 2, 3, 4, respectively. In the two first cases, since we know the exact formula (11) for ξ_∞, in which appears $L-2$, we have plotted ξ^2/ξ_∞^2 as a function of $t/(L-2)^\gamma$. In the third case, since there is no reason to use $L-2$ instead of L, we have plotted ξ^2/L as a function of t/L^γ. These plots allow us to appreciate the finite size corrections to scaling. These corrections increase when going from the first to the third case. This is consistent with the increasing slopes for the corresponding effective γ_L exponents observed in figure 5. We were unable to do the same for the entropy and we did not find a reasonable scaling form, especially in the ballistic case, where the L-dependence of s_∞ cannot be determined.

5. Conclusion

In this paper, we have presented a simple finite-size scaling method well adapted to investigate surface growth models with restricted step heights. The method can simply be extended to other two-dimensional studies such as the effect of a tilted baseline [15], by considering states with finite magnetization, or to the Kim-Kosterlitz case [13], by considering spins 1 instead of spins $\frac{1}{2}$ etc.... We also intend to extend the method to three dimensions. Even if this extension will be much more computer time consuming, we think it will be very interesting to compare the results with Monte Carlo data, especially after the recent numerical evidences that crossovers of the type studied here can become true phase transitions in three dimensions [16].

Acknowledgments

We thank Y P Pellegrini, L Sander and P Meakin for discussions. Numerical calculations were done at CIRCE (Centre Inter-Régional de Calcul Electronique), Orsay, France.

References

[1] Vold M J 1959 *J. Colloid and Int. Science* **14** 168; 1959 *J. Phys. Chem.* **63** 1608; 1960 *J. Phys. Chem.* **64** 1616

[2] Eden M 1961 *Proc. Fourth Berkeley Symp. on Math. Stat. and Prob.* vol IV, ed F Neyman (Berkeley, CA: University of California Press)

[3] Family F and Landau D P 1984 *Kinetics of Aggregation and Gelation* (Amsterdam: North-Holland) Stanley H E and Ostrowski N 1985 *On Growth and Forms, a Modern View* (Deventer: Kluwer) Jullien R and Botet R 1987 *Aggregation and Fractal Aggregates* (Singapore: World Scientific)

[4] Meakin P 1987 *CRC Crit. Rev. Solid State Mat. Sci.* **13** 143
[5] Meakin P, Ramanlal P, Sander L M and Ball R C 1986 *Phys. Rev.* A **34** 5081
[6] Meakin P and Jullien R 1987 *J. Physique* **48** 1651
[7] Family F and Vicsek T 1985 *J. Phys. A: Math. Gen.* **18** L75
[8] Family F 1986 *J. Phys. A: Math. Gen.* **19** L441
[9] Plischke M, Racz Z and Liu D 1987 *Phys. Rev.* B **35** 3485
[10] Edwards S F and Wilkinson D R 1982 *Proc. R. Soc.* A **381** 17
[11] Kardar M, Parisi G and Zhang Y C 1986 *Phys. Rev. Lett.* **56** 889
[12] Barber M N 1983 *Phase Transitions and Critical Phenomena* vol 8, ed C Domb and J L Lebowitz (New York: Academic).
[13] Kim J M and Kosterlitz J M 1989 *Phys. Rev. Lett.* **62** 2289
[14] Dhar D 1987 *Phase Transitions* **9** 51
[15] Krug J 1989 *J. Phys. A: Math. Gen.* **22** L769
[16] Amar J G and Family F 1990 *Phys. Rev. Lett.* **64** 543
Yan H, Kessler D and Sander L M 1990 *Phys. Rev. Lett.* **64** 926
Pellegrini Y P and Jullien R 1990 *Phys. Rev. Lett.* **64** 1745
[17] Kardar M and Zhang Y C 1986 *Phys. Rev. Lett.* **58** 2087 1987
[18] Halpin-Healy T 1989 *Phys. Rev. Lett.* **62** 442